Journal of Structural Geology, Vol. 8, No. 1, pp. 3–14, 1986
Printed in Great Britain

0191-8141/86 $3.00 + 0.00

Implications of mylonitic microstructures for the geotectonic evolution of the Median Tectonic Line, central Japan

HIDEO TAKAGI

Institute of Earth Science, School of Education, Waseda University, Shinjuku, Tokyo, 160 Japan

(*Received* 4 *September* 1984; *accepted in revised form* 23 *April* 1985)

Abstract—The Median Tectonic Line (MTL), the most prominent onshore fault in Japan, demarcates the Cretaceous Hiji quartz dioritic gneiss of the Ryoke belt on the west from the high P/T type Sambagawa metamorphic rocks on the east in the Takato area. Toward the MTL, the Hiji gneiss grades into strongly mylonitized rocks characterized by grain-size reduction of quartz. In the mylonitic rocks, the development of fluxion banding (Sm) is remarkably influenced by the existence of K-feldspar, forming a myrmekitic intergrowth. Brittle microstructures indicative of truly cataclastic deformation are observed only in mylonitic rocks close to the MTL. Early deep-level ductile deformation apparently gave way to shallower, brittle deformation at a later stage. The attitude of stretching lineations (Lm) and asymmetric microstructures observed in the mylonites suggest that sinistral strike-slip shearing with a subordinate component of vertical-slip took place during mylonitization in mid-Cretaceous time. The mylonitic rocks and their protolith, supposed to have constituted the eastern limb of the shear zone, were probably eroded out and lost by upheaval of the Sambagawa belt relative to the Ryoke belt.

INTRODUCTION

THE MEDIAN Tectonic Line (MTL) is a major tectonic feature dividing southwest Japan into Inner (northern) and Outer (southern) zones. It has a strike length of nearly 1000 km, and is the longest fault in Japan. The MTL forms the boundary between two contrasting metamorphic belts; one is a low P/T belt of cordierite–sillimanite rocks closely associated with granitic rocks in the north (Ryoke belt), and the other is a high P/T glaucophane-bearing belt of crystalline schists in the south (Sambagawa belt). The two belts are examples of 'paired metamorphic belts' (Miyashiro 1961). From the western half of the Kinki district westward, the Izumi Group of Upper Cretaceous marine sediments unconformably covers the Ryoke metamorphic rocks and granites, and is in contact with the Sambagawa belt along the MTL (Fig. 1).

In the Chubu and the Kinki districts, a mylonite zone, several hundreds to a thousand meters in width, is developed along the MTL in the Ryoke belt. Some subsidiary mylonite zones, branching off from the major zone along the MTL, are known in the Kinki district (Hara *et al.* 1980).

The mylonitic rocks along the MTL in the Takato area have been studied by many geologists from the viewpoint of their petrogenesis, parent rocks, structural relationship to the MTL, and other features (e.g. Sugiyama 1939, Hashimoto 1957, Hayama *et al.* 1963, Hayama & Yamada 1980, Ono 1981). Recently, the writer made a detailed geological and petrographical study of the mylonitic rocks in this area re-examining the above-mentioned problems. Part of the results have already been reported (Takagi 1983, 1984). From microfabric analyses of the mylonitic rocks in the Chubu and Kinki districts, Hara *et al.* (1977, 1980) proposed a movement-strain picture of a ductile shear zone during mylonitization. Kosaka (1980) described many ductile–brittle microstructures of the mylonitic rocks along the MTL in the Kinki district and along other major faults, and estimated physical conditions of deformation by comparison with high-temperature deformation experiments on quartz aggregates. Except for these preliminary studies, there are few contributions for the tectonic setting and deformation mechanisms of mylonitic rocks along the MTL. The geometry of tectonic movement at

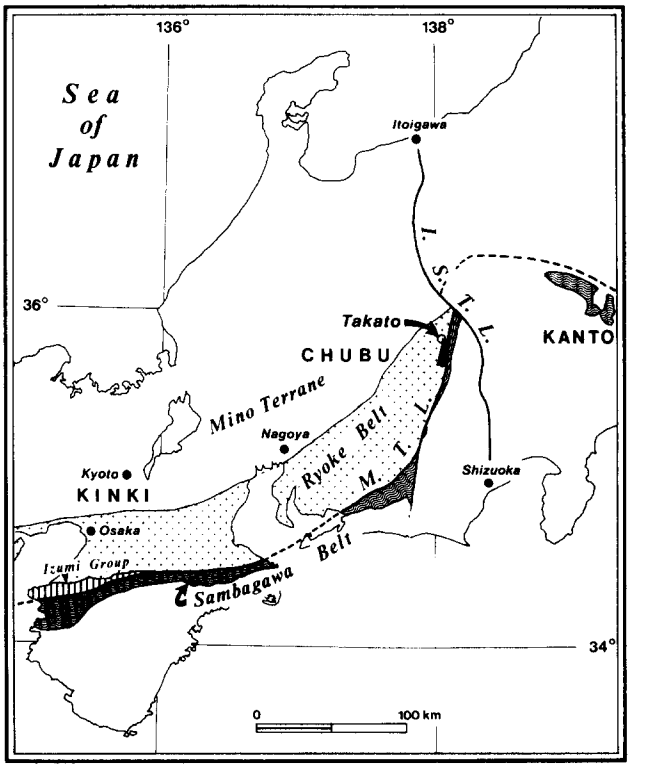

Fig. 1. Regional setting of the Median Tectonic Line (MTL) and paired metamorphic belts in central Japan. Location of study area (black) is indicated. I.S.T.L., Itoigawa–Shizuoka Tectonic Line.

the stage of mylonitization has not yet been revealed. With some review of the previous papers written in Japanese (Takagi 1982, 1983, 1984), the present paper describes the meso- and microstructural features of the mylonitic rocks, the asymmetric microstructures in the mylonitic rocks as an indicator of the sense of shearing, and discusses the deformation history of the mylonitic rocks and the tectonic relationship between the mylonitic rocks and the MTL.

GEOLOGICAL AND STRUCTURAL SETTING

The MTL runs approximately N–S, dipping vertically in the Takato area. To the north of this area, the MTL is offset by the Itoigawa–Shizuoka Tectonic Line (I.S.T.L., Fig. 1) bounding the western margin of the 'Fossa Magna', a major graben-like rupture zone. Outcrops of the MTL displaying direct tectonic contact between the Ryoke and the Sambagawa belts, are known at six locations where incohesive fault gouge is lacking.

The Sambagawa belt in the Takato area is composed mainly of quartzose pelitic schist with subordinate amounts of basic schist. The schists strike nearly parallel, or in places a little oblique, to the MTL and dip to the east at moderate angles. A spotted schist, characterized by albite porphyroblasts visible to the naked eye, forms a narrow zone nearly parallel to the MTL (Fig. 2), (Kawachi *et al.* 1983).

From west to east the Ryoke belt in the Takato area is composed of (1) Ryoke metamorphic rocks, (2) massive quartz diorite (Katsuma quartz diorite) and (3) quartz dioritic gneiss (Hiji gneiss) (Fig. 2).

The Ryoke metamorphic rocks are mostly psammitic and pelitic rocks (schistose hornfels, gneiss and migmatite). Toward the west–northwest, normal to the general structural trend of the rocks, they grade into weakly metamorphosed Jurassic sediments in the Mino terrane. Based upon the radiometric age data together with geologic evidence, the regional metamorphism and following emplacement of the 'Older Granites' in the Ryoke belt are inferred to take place in mid-Cretaceous (*c.* 90–110 Ma). However, the K–Ar age of the metamorphic rocks is 60–70 Ma, interpreted as the age of a rejuvenation by widespread intrusion of the 'Younger Granites' (Ischizaka 1966, Tanaka & Nozawa 1977).

The Katsuma quartz diorite is a coarse-grained massive hornblende–biotite quartz diorite. This elongate plutonic mass, only 1 km in width, extends N–S for about 20 km. It was emplaced concordantly in the Ryoke metamorphic belt. The Katsuma quartz diorite is situated very near to the MTL to the north of Takato, but no mylonitization has been recognized in it. The Rb–Sr mineral age of biotite in the diorite is 83 Ma (Hayase & Ishizaka 1967).

The Hiji quartz dioritic gneiss is the oldest of the granitic rocks in the Ryoke belt (Ryoke Research Group 1972). It extends over 30 km from north to south with a width of 1–4 km in the study area. To the south of the Bungui Pass, most of the Hiji gneiss has been transformed into mylonitic rocks in a narrow zone along the MTL (Hayama *et al.* 1963, Hayama & Yamada 1980). The Hiji gneiss consists always of quartz, plagioclase (An 35–40), ±K-feldspar (microcline), biotite,

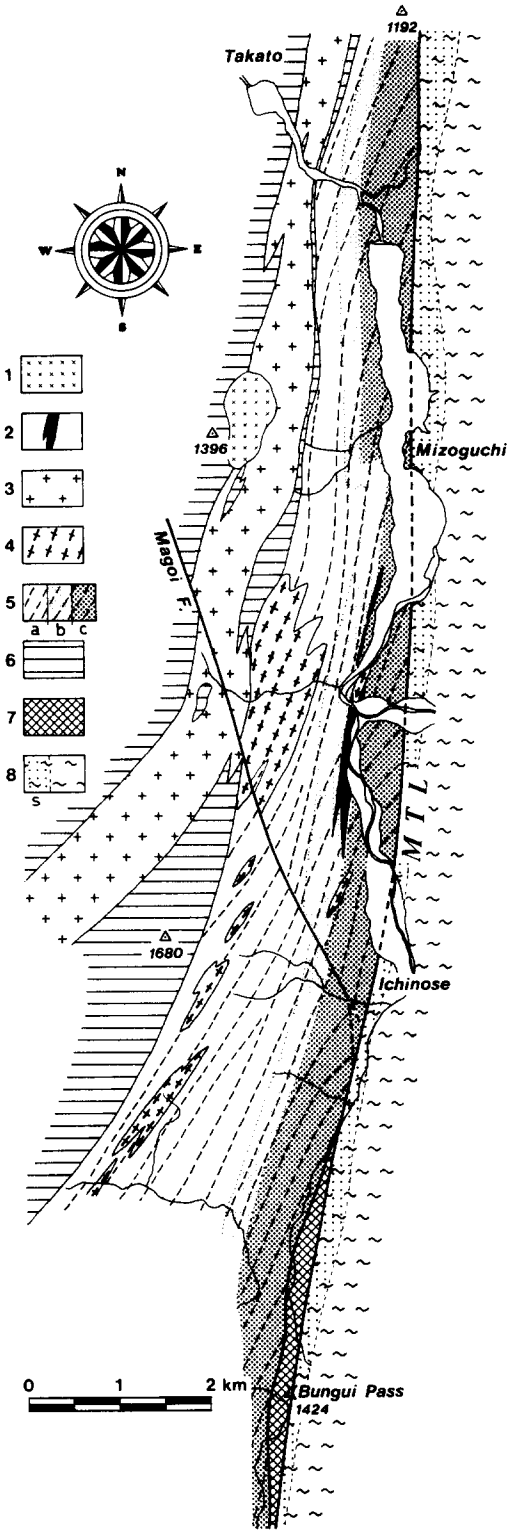

Fig. 2. Geological map of the Ryoke belt along the MTL, south of Takato area, simplified and partly modified after Takagi (1984). 1, granite; 2, hornblende diorite; 3, Katsuma quartz diorite; 4, Minakata granodiorite; 5, Hiji quartz dioritic rocks (a: gneiss, b: mylonitic gneiss, c: blastomylonites and mylonites); broken lines show the trace of foliations (*Sg*/*Sm*); 6, Ryoke metamorphic rocks; 7, Schistose microbreccia (psammitic gneiss); 8, Sambagawa crystalline schists (s: spotted zone).

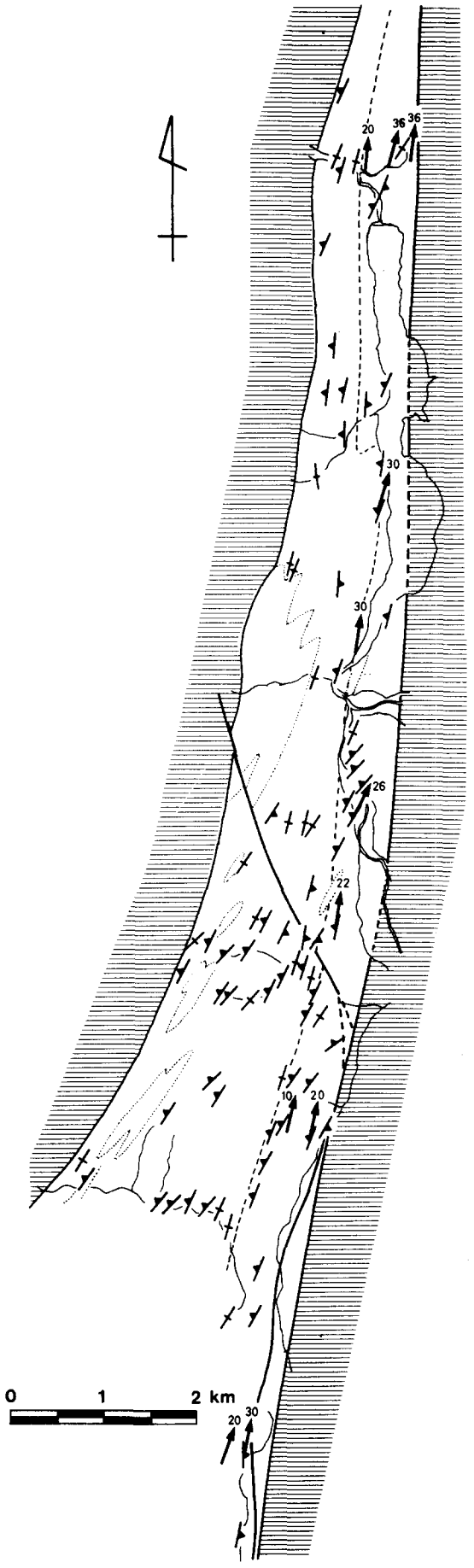

Fig. 3. Structural map showing foliation (*Sg* and *Sm*) of gneisses and mylonitic rocks, and stretching lineation (*Lm*, arrows) of mylonitic rocks. A fine broken line shows the western margin of the M zone (see Fig. 5).

hornblende, with accessories of sphene, allanite, epidote, zircon and apatite, but is remarkably heterogeneous, varying in proportion of the constituent minerals and in their grain size. It locally possesses a conspicuous banded structure. Banded gneiss occupies the middle zone of the gneiss body, and its structure trends subparallel to the MTL. The mineral assemblage of the gneiss is rather uniform. Intrafolial folds and other migmatitic structures occur locally. Gneissosity (*Sg*) strikes 010–040°, and dips vertically or steeply to the west. It forms a 10–30° southward-opening angle with the N–S trending MTL (Fig. 3). Whole-rock Rb–Sr isotopic ages of the Hiji gneiss are widely dispersed, ranging between 265 and 110 Ma (Kagami 1973). Recently Yamana *et al.* (1983) reported a whole rock Rb–Sr age of 90 Ma for the specimens taken from some selected parts of the Hiji gneiss. Although the age of emplacement of the Hiji gneiss remains unfixed, it is considered to be mid-Cretaceous (*c.* 100 Ma) since it was emplaced concordantly in the Ryoke metamorphic rocks.

Lenticular bodies of a coarse-grained gneissose granodiorite (Minakata granodiorite) have been intruded locally into the Hiji gneiss. Near the MTL, these rocks have been weakly mylonitized to exhibit typical 'augen' gneiss characteristics.

Towards the MTL, the Hiji gneiss apparently grades into the mylonites. Comparison of the mineral and chemical composition and field observation of the transition between the two types of rocks reveal that most of the mylonitic rocks along the MTL have originated through mylonitization of the Hiji gneiss (Takagi 1984). Xenolithic lenses of micaceous or quartzose phyllonites of metasedimentary origin are also locally present in the mylonite zone.

MESOSCOPIC STRUCTURES

The mylonitic rocks frequently exhibit mylonitic foliation (*Sm*). *Sm* is defined by a dimensional preferred orientation of elliptical porphyroclasts and fluxion banding characterized by elongate pressure shadows (Fig. 4). The thickness of the fluxion banding ranges from 0.1 to 1 mm, thinner than that of the original compositional banding (*Sg*). Sm is commonly parallel to *Sg* and is thought to nearly parallel the *XY* plane of the finite strain ellipsoid. Intrafolial folds are occasionally observed in the banded mylonites where the flattening plane of the porphyroclasts is nearly parallel to the axial plane of the folds. Close to the MTL, the strike of *Sg* and *Sm* tends to rotate clockwise (Figs. 2 and 3). The stretching lineation (*Lm*) is defined by the *X* direction on the *XY* plane (*Sm*) (Figs. 4a & c). *Lm* measured on the foliated mylonitic rocks plunges N–NNE at 20–30° (Fig. 3).

Close to the MTL, the above-mentioned *L–S* fabric has been disrupted by post-mylonitic brittle deformation (Takagi 1983). Strongly deformed cataclasites occur immediately adjacent to the MTL and to other faults

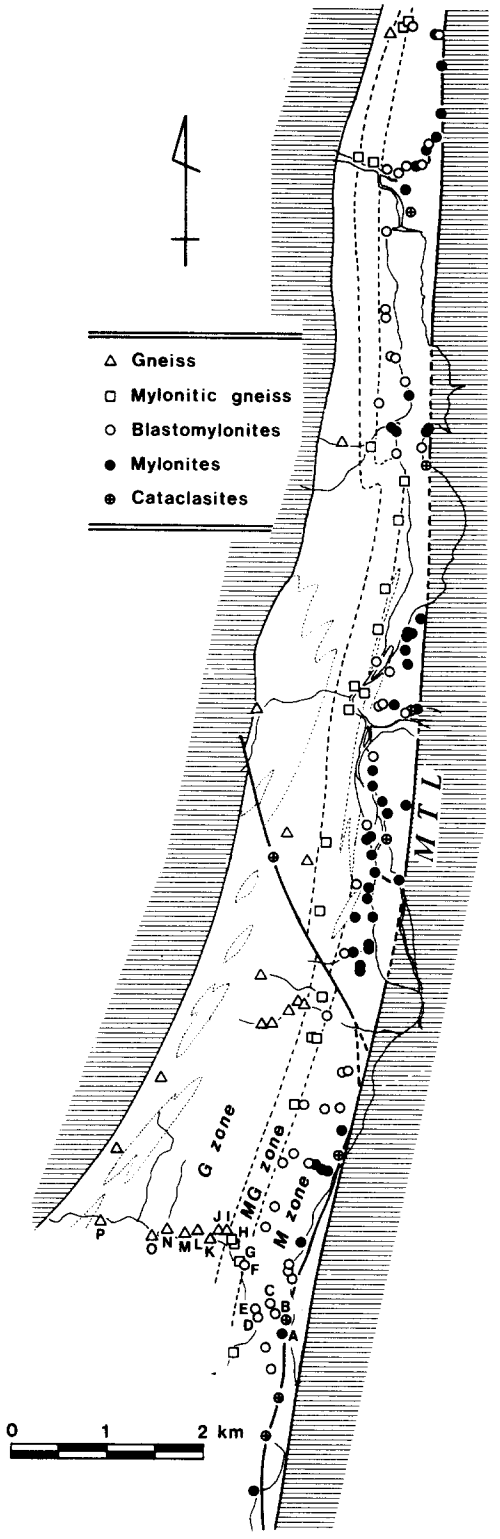

Fig. 5. Distribution of gneisses and mylonitic rocks on the basis of the classification shown in Table 1 partly modified after Takagi (1984). Initials (A–P) show the location of specimens for analyses of the grain size and the aspect ratio of recrystallized quartz grains (see Fig. 6). The zones of 'G', 'MG' and 'M' signify those of gneiss, mylonitic gneiss and mylonites–blastomylonites, respectively (see Table 1).

(Fig. 5). Irregular veins filled with calcite, prehnite and K-feldspar are widespread there. At the Bungui Pass and in its vicinity, a strongly crushed zone occurs close to the MTL. It consists mainly of a schistose microbreccia derived from psammitic gneiss with small bodies of tectonically intercalated Sambagawa schist.

DEFORMATION–RECRYSTALLIZATION MICROSTRUCTURES

Classification of mylonitic rocks

The classification and terminology of mylonitic rocks in this paper follows that of Takagi (1982) (Table 1). It is modified from the classifications proposed by Higgins (1971) and Sibson (1977) to avoid genetic connotations. Mylonite-series rocks are commonly classified into three gradational types: protomylonite–mylonite–ultramylonite, and it has been described in many shear zones that the proportion of porphyroclasts reduces as mylonitization becomes stronger. In the study area, however, the Hiji gneiss, a protolith of mylonites, is extremely heterogeneous in mineral content and texture, such that alternating layers of 'protomylonite' and 'ultramylonite' are commonly observed. It is unacceptable, here, to use the prefixes proto- and ultra- which imply a grade of mylonitization. Thus the writer makes a two-fold descriptive division of mylonites into P-mylonite and F-mylonite, used in addition to the term blastomylonites. The maximum grain size of quartz tentatively defines the border between mylonites and blastomylonites (0.1 mm), and that between blastomylonites and mylonitic gneiss (0.4 mm).

Mixed ductile–brittle deformation microstructures in each mineral and whole rock are summarized in Table 2 following detailed descriptions by Takagi (1983, 1984).

Grain-size reduction of quartz

The commonest feature of mylonitic rocks is a grain-size reduction of the constituent minerals, compared with the surrounding parent rocks. This by itself constitutes one of the definitions of a 'mylonite' (Bell & Etheridge 1973). The most sensitive mineral for grain-size reduction is quartz, which constitutes a major component of the matrix and contributes to the ductile behaviour of mylonites. On the basis of the maximum recrystallized grain size of quartz, the Hiji quartz dioritic body is divided into three zones in order of increasing deformation towards the MTL: G (gneiss) zone, MG (mylonitic gneiss) zone and M (blastomylonites and mylonites) zone (Fig. 5 after Takagi 1984). The mylonite-zone wall is nearly parallel to the MTL. The grain sizes are re-examined after Takagi (1984 fig. 7B) in each section in which individual grains were selected exclusively from polycrystalline pods or elongated lenses to avoid grain-size control by the other phases on grain boundaries (e.g. Etheridge & Wilkie 1979). Quartz grains infilling extension cracks were excluded from the measurement. The mean grain size is defined by

$$\bar{s} = \left(\prod_i a_i b_i \right)^{1/n},$$

where a_i is the long diameter, b_i is the short diameter and $n = 200$. Figure 6(a) indicates $\bar{s}$ in relation to the distance, D, from the MTL. It shows that the effects of mylonitization extend up to 1500 m west from the MTL.

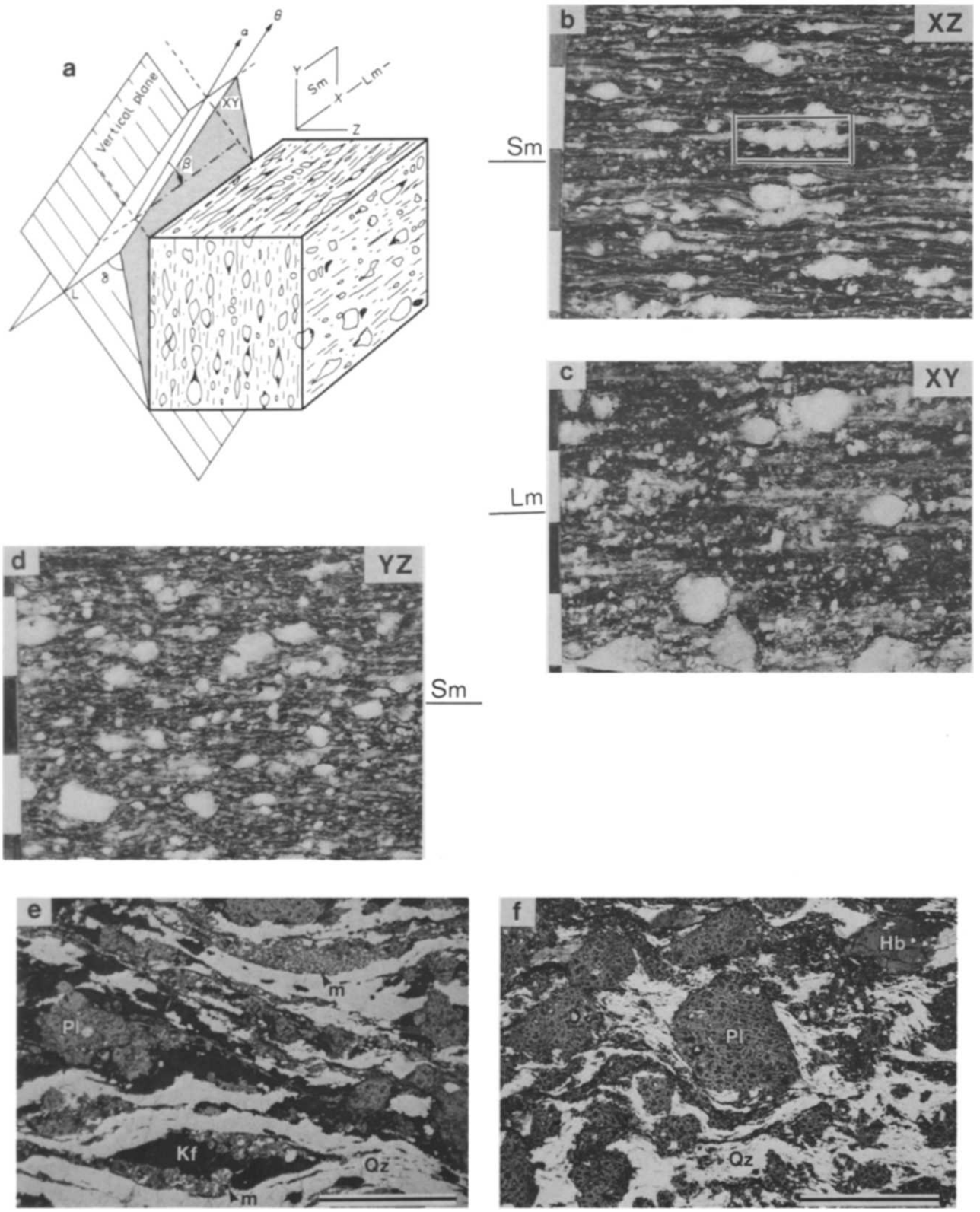

Fig. 4. (a) Geometrical illustration of typical foliated mylonite, (b)–(d) polished rock slices of each section; (b) XZ section; boxed part shows displaced broken grains indicating sinistral shear, (c) XY section (Sm) and (d) YZ section. θ: strike of foliation (Sm) and $010° < \theta < 040°$; α: trend of lineation (Lm), $0° < \alpha < 030°$; δ: dip of foliation, $\delta = 70$–$90°$ west; β: plunge of lineation, $\beta = 20$–$30°$ north. (e) Fluxion banding developed in K-feldspar-bearing blastomylonite, m, myrmekitic intergrowth; Kf, K-feldspar; Qz, quartz. Thin section stained, PPL, Bar scale 1 mm. (f) P-mylonite without K-feldspar. Fluxion banding cannot be seen. Pl, Plagioclase; Hb, Hornblende. Thin section stained. PPL, Bar scale 1 mm.

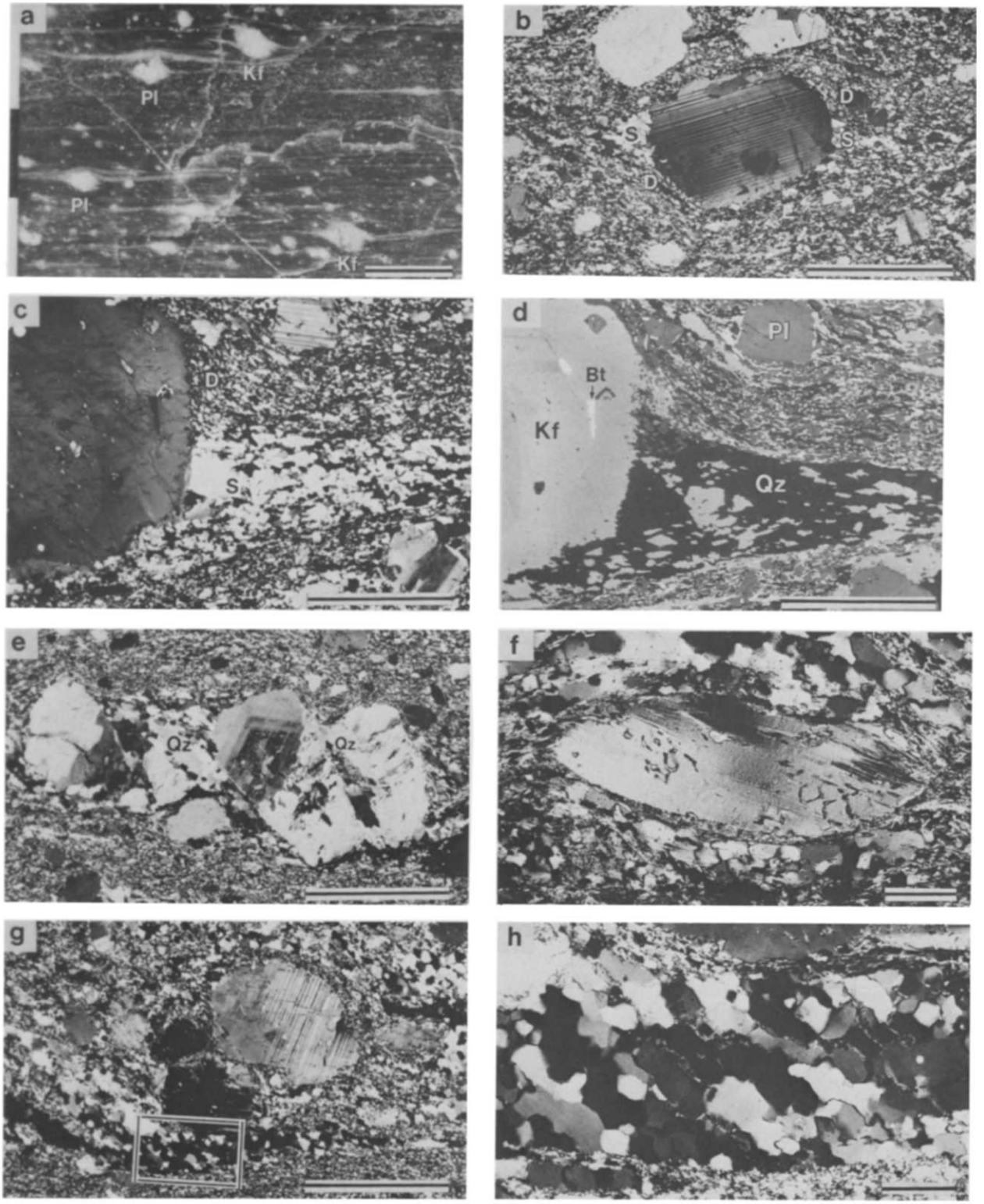

Fig. 7. Asymmetric microstructures in F mylonites (a)–(e), in phyllonite (f) and in blastomylonite (g) & (h). (a) Asymmetric pressure shadows on both sides of porphyroclasts of plagioclase and K-feldspar, polished rock slice. Bar scale 1 cm. (b) Plagioclase porphyroclast with pressure shadow 'wings' (S) and dragged parts (D). XPL, Bar scale 1 mm. (c) K-feldspar porphyroclast with pressure shadow (right wing) and dragged part. XPL, Bar scale 1 mm. (d) Compositional image photograph taken by the EPMA (JXL733), the same part as shown in (c). Note the aggregation feature in pressure shadow (quartz and K-feldspar) and in matrix (quartz, plagioclase, K-feldspar and biotite). Bt, biotite. Bar scale 1 mm. (e) Displaced broken grains of plagioclase in ductile matrix. Most grains are more or less pulled apart with infilled quartz (Qz). XPL, Bar scale 1 mm. (f) Muscovite 'fish' in phyllonite. The (001) cleavage tilted 20° back against the sense of shear and partly distorted and disrupted. XPL, Bar scale 0.1 mm. (g) Recrystallized grains of quartz and K-feldspar with their flattening plane oblique to the fluxion banding (*Sm*) parallel to the long axis of the photograph. XPL, Bar scale 1 mm. (h) Magnification of the boxed area in (g). XPL, Bar scale 0.1 mm.

Table 1. Classification of mylonitic rocks after Takagi (1982)

Vol % of fragments	Incohesive	Cohesive			vol % of porphyroclasts
		Nature of matrix: Tectonic reduction in grain size predominates	(Max. size of quartz <0.1 mm)	Grain growth pronounced (>0.1 mm)	
>30%	Fault breccia	Microbreccia } CATACLASITES	P-Mylonite } MYLONITES	Mylonite gneiss } BLASTOMYLONITES	
<30%	Fault gouge	Cataclasite } CATACLASITES	F-Mylonite } MYLONITES	Blastomylonite } BLASTOMYLONITES	
	Random-fabric (with crushing)		Foliated (with recrystallization)		

P, 'Porphyroclastic'.
F, 'Flinty'.

Table 2. Common deformation features of each mineral and whole rock in mylonites–blastomylonites and in cataclasites

	Mylonites–Blastomylonites	Cataclasites
Quartz	Undulatory extinction (weak-moderate)	Undulatory extinction (strong) Deformation bands Deformation lamellae
Plagioclase	Bending Glide twinning Extension cracks	Microfaults Kink bands Deformation bands Healed fractures
K-feldspar	Undulatory extinction	Undulatory extinction Extension cracks Deformation bands Healed fractures
Biotite	Bending	(Altered to chlorite)
Hornblende	Bending Kinking Extension cracks	(Altered to chlorite and calcite)
Allanite	Bending Kinking Extension cracks	Granulation Comminution
Whole rock	Fluxion structure Fluxion banding Pressure shadows Shear bands	Fracture Veining Kink bands Granulation

Table 3. Schematic diagram of time sequence and conditions for formation of mylonitic rocks. The strain rates given are those commonly used in discussions dealing with the formation of mylonitic rocks (White 1975, Sibson 1977, Watts & Williams 1979) and generation depth and temperature are taken from Sibson (1977)

Time	Regime	Deformation mode	Deformation product	Fabric	Width of def. zone	Generation depth	Strain rate
↑	Elastico-frictional	Brittle fracture	—	Incohesive random	1 m	1–4 km	(sec)
		Cataclasis	Cataclasites	Cohesive random	100 m	4–10 km	10^{-3}/sec (min)
	Transitional					10–15 km (250–350°C)	
	Quasi-plastic	Mylonitization	Mylonites Blastomylonites	Fluxion banding(Sm)	1 km	15–20 km	10^{-12}–10^{-14}/sec (Ma)
		Metataxis?	Migmatitic gneiss	Compositional banding (Sg)	?	?	?

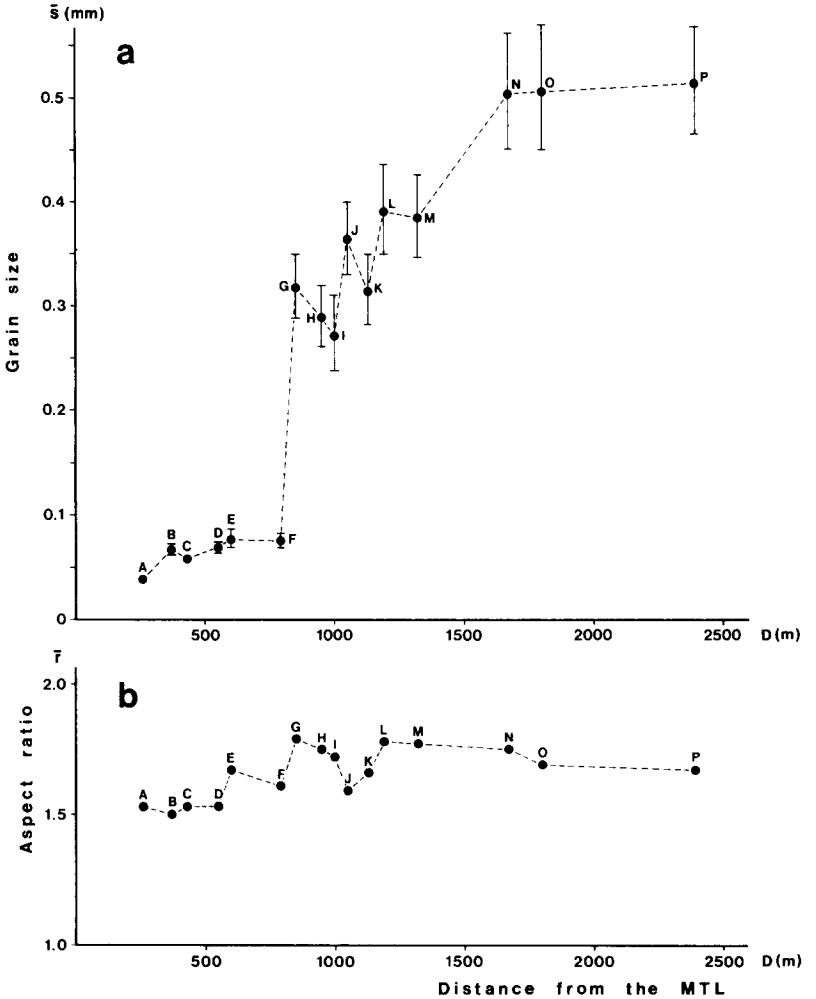

Fig. 6. (a) Relationship between the geometric mean grain size (s) of recrystallized quartz and the distance (D) from the MTL. Limit bars represent 95% confidence interval. (b) Relationship between the mean aspect ratio (r) of recrystallized quartz and the distance from the MTL. Initials (A–P) are the same as those shown in Fig. 5.

In the M zone, which lies nearest to the MTL (Fig. 5) with its western limit about 800 m from the MTL, the mean size of quartz falls below 0.1 mm. The mean aspect ratio is defined by

$$\bar{r} = \frac{1}{n}\left(\sum_{i} a_i/b_i\right).$$

Figure 6(b) shows $\bar{r}$ in relation to D. Although the ratio tends to decrease slightly toward the MTL, no marked change is observed. The shape of quartz is essentially equidimensional and polygonal, correlating with the P-type quartz defined by Masuda & Fujimura (1981) (see Figs. 7c, f & h).

Role of K-feldspar for development of mylonitic fabrics

A remarkable feature of the foliated mylonitic rocks as well as the grain-size reduction of quartz is the important role K-feldspar plays in controlling the development of fluxion banding closely related to the formation of fine-grained myrmekitic aggregates. In the mylonitic gneiss and blastomylonites, myrmekitic aggregates of plagioclase, quartz and minor K-feldspar mantle K-feldspar porphyroclasts and extend along the matrix foliation away from the host grain as tails which alternate with stretched aggregates of recrystallized quartz (Fig. 4e). This alternation defines the typical fluxion banding and develops especially in the blastomylonite. Quartz grains within the tails of myrmekitic aggregates preserve their drop-like or worm-like shapes and their diameters range from 5 to 30 μm. In fine-grained mylonites, myrmekite is rare or lacking.

The matrix of K-feldspar-bearing mylonites constitutes large amounts of irregular, fine-grained plagioclase and K-feldspar together with quartz grains and mica flakes (Fig. 7d). Quartz grains in such a 'mixed' matrix are moderately rounded and fine grained (<20 μm), and often exhibit undulatory extinction. On the other hand, mylonitic rocks devoid of K-feldspar (namely without myrmekite) are dominantly composed of recrystallized quartz with minor amount of phyllosilicates in a matrix lacking fluxion banding (Fig. 4f). On this basis, it appears that the fine-grained aggregates of plagioclase, K-feldspar, quartz and mica in the matrix of the mylonites formed as a consequence of the above-mentioned myrmekitic intergrowth. A highly ductile behaviour of the trails of such aggregates may be inferred from the model for grain arrangement during superplastic flow

(Kerrich *et al.* 1980). Pressure shadows composed of larger polygonal grains of quartz and/or K-feldspar on both sides of porphyroclasts develop exclusively in K-feldspar-bearing mylonites (Figs. 7b–d). Their presence in coexistence with a 'mixed' matrix suggests that the deformation took place accompanying intercrystalline diffusive mass transfer (Elliott 1973). It has been pointed out in many studies that the formation of myrmekitic or fine-grained aggregates in the mantle of K-feldspar porphyroclasts is probably induced by deformation (e.g. Shelley 1964, Hanmer, 1980).

ASYMMETRIC MICROSTRUCTURES

Several types of asymmetric microstructures (showing monoclinic symmetry) described recently by Simpson & Schmid (1983) and Lister & Snoke (1984) are observable in the *XZ* sections of the foliated mylonitic rocks in the study area. Those microstructures, considered to be useful to deduce the sense of shearing, include asymmetric pressure shadows, displaced broken grains, mica 'fish' and oblique incremental quartz elongation fabrics. The first two are also observable in outcrops or polished rock slices (Figs. 4b and 7a). There has been no previous description of such microstructures in foliated mylonitic rocks along the MTL. The orientation of the mylonitic foliation (*S*m) approaching the MTL (Fig. 2) displays less convincing macroscopic evidence for shear displacement (Ramsay & Graham 1970) than the microscopic evidence described below. A detailed description and fabric analysis of the asymmetric microstructures are being undertaken at present (Takagi & Ito 1985).

Asymmetric pressure shadows

In foliated mylonitic rocks, asymmetric pressure shadows commonly occur as 'wings' of a rigid feldspar porphyroclast (Figs. 7a–d). Figure 8(a) shows the asymmetric drag pattern made by an experimental study for the case of sinistral simple shear parallel or at a low angle to the pre-existing foliation (partly modified from Ghosh 1975, fig. 4). A similar asymmetric pattern is also demonstrated by the disturbance of strings outside a rotated ring ('string model' of Schoneveld 1977). A predominance of pressure shadows displaying the asymmetry with respect to the mylonitic foliation shown in Fig. 8(a) suggests that the shear sense during mylonitization was sinistral.

Displaced broken grains

Extension cracks in rigid porphyroclasts (mostly of plagioclase) are frequently observed in the foliated mylonitic rocks. They generally appear nearly normal to both *L*m and *S*m, and some of them, especially in the highly foliated mylonitic rocks, are oriented oblique to *S*m in their *XZ* section, accompanying a rotation of broken grains. Although the cracks appear opened on both sides with infilled quartz, the rotation of grains is

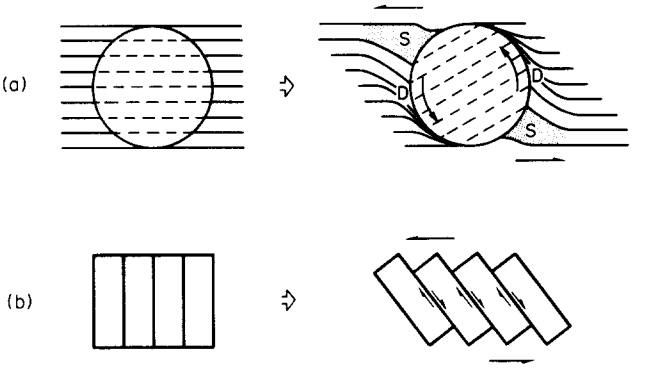

Fig. 8. Schematic illustrations of models of vorticity for deduction of the sense of shear. (a) Drag pattern of passive markers around a rigid spherical body (after Ghosh 1975). Marker lines were initially parallel to the shear direction during simple shear. D, dragged area; S, pressure shadow area. (b) The sheared stack of cards model applicable to the broken and displaced hard grains.

analogous to a sheared stack of cards model (Fig. 8b) (Simpson & Schmid 1983, after Etchecopar 1974, 1977). From this model, the displaced broken grains of plagioclase indicate a sinistral sense of shearing (Figs. 4b and 7e).

Mica 'fish'

Phyllonite of metasedimentary origin commonly contains spindle-shaped muscovite porphyroclasts (Takagi 1982). These have been called mica 'fish' and used to indicate the sense of shear (Lister & Snoke 1984). The (001) cleavage of mica 'fish' are usually inclined at 10–30° to *S*m as shown in Fig. 7(f), giving a sinistral sense of shear.

Oblique incremental quartz elongation fabric

The shape of recrystallized quartz grains in pressure shadows is fairly equant. However, when the grains are included in stretched layers or lenses apart from the pressure shadows, they occasionally show an elongate fabric oblique to *S*m (Figs. 7g & h). Simpson & Schmid (1983) suggest that oblique, elongated, recrystallized grains of quartz make it possible to deduce the sense of shear. Again, a sinistral sense of shear is deduced.

DISCUSSION

In the Takato area, tectonic movements affecting the Ryoke plutonic body along the MTL can be divided into three successive major stages: (1) syn-tectonic emplacement of the Hiji gneiss (metatexis), (2) sinistral ductile shearing (mylonitization) and (3) brittle fault movement (cataclasis) (Table 3).

Syntectonic emplacement of the Hiji gneiss

The Hiji gneiss has been considered as the product of migmatization (granitization) of basic rocks (e.g. biotite amphibolite) defined as metatexis or metablastesis

(Hashimoto 1957, Kanisawa 1961). Migmatization took place at temperatures equivalent to the lower grade of amphibolite facies (Kanisawa 1961). As already stated, the foliation (Sg) in the banded facies of the Hiji gneiss tends to strike more concordantly with the trend of the MTL than that of the relatively massive facies, giving the appearance of a sinistral shear zone. This suggests that the gneissose structure, especially the intense migmatitic banding, was produced by strain localized in weaker facies. Syntectonic emplacement of the Hiji gneiss was followed by mylonitization resulting from sinistral ductile shearing.

Geometry and shear sense of the ductile shear zone

Asymmetric pressure shadows and three other microstructures described in this paper all indicate sinistral shearing in foliated mylonitic rocks along the MTL. The same sense of shearing along the MTL can be deduced from other evidence; the trajectories of the longest principal axis (X) of strain ellipsoids based on the incremental quartz elongation fabric (Hara *et al.* 1977, 1980). Many authors have considered that in the highest strain portions of shear zones, the stretching lineation in the mylonitic foliation (XY plane) approximates the shear direction (e.g. Berthé *et al.* 1979, Watts & Williams 1979, Sibson *et al.* 1981). As already mentioned, the stretching lineation (Lm) in the mylonitic rocks plunges NNE at 20–30°. Consequently, it is concluded that the shear movement forming the mylonite zone in the Takato area was dominantly sinistral strike-slip with a minor vertical-slip component uplifting the western side of the shear zone relative to the eastern.

Cataclastic deformation

Cataclastic deformation characterized by brittle fragmentation has been imprinted on the foliated mylonitic rocks immediately adjacent to the MTL. As listed in Table 2, features of this cataclastic deformation can be easily discriminated from those of the ductile deformation for each mineral and for the whole rock. Such cataclastic microstructures are also found in the Sambagawa crystalline schists close to the MTL (Takagi 1983). Thus, the cohesive cataclastic deformation can be attributed to an upper-crustal fault movement of the MTL under the elastico-frictional (EF) regime defined by Sibson (1977) (see Table 3). Incohesive fault gouge is almost lacking in the outcrops of the MTL in the study area (Takagi 1983). This suggests that the MTL in the area has not been active recently as suggested by Kawachi *et al.* (1983) on the basis of geomorphological observation.

Interpretation of the geotectonic history of the MTL

The following points are critical in considering the geotectonic relation between the mylonitic rocks and the MTL.

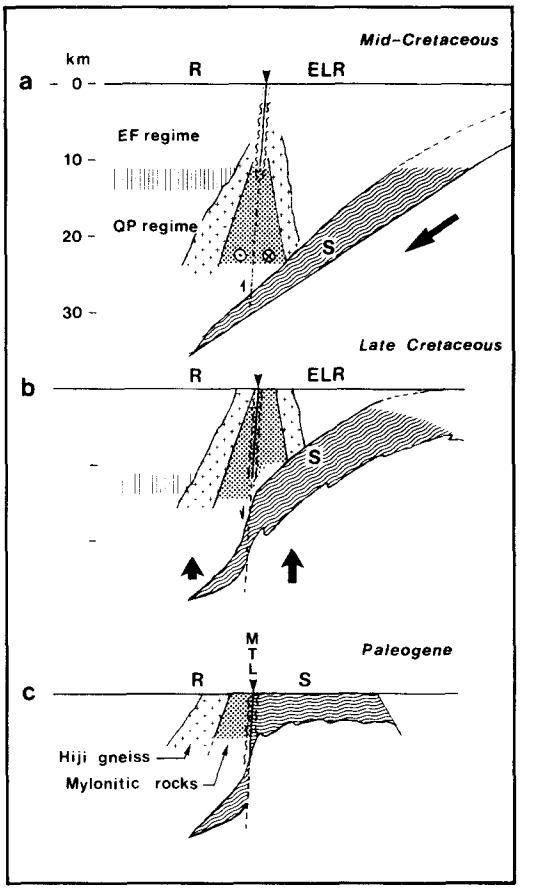

Fig. 9. Schematic illustrations of tectonic setting of the mylonitic rocks combined with the model of the tectonic generation of the MTL proposed by Ichikawa (1970). R, Ryoke belt; ELR, eastern limb of the Ryoke belt. S, Sambagawa metamorphic rocks. See text.

(1) The foliation (Sm) and lineation (Lm) of the mylonitic rocks trend obliquely, though at a low angle (10–30°), to the MTL.

(2) No evidence of intense mylonitization has been found to date in the Sambagawa crystalline schists.

(3) The axis of the thermal structure obtained from isograds in the metamorphic rocks of the Ryoke belt is cut discordantly by the MTL. This suggests that the MTL is a contact of two contrasting metamorphic belts, generated after the Ryoke regional metamorphism ended (Suwa 1973).

(4) The MTL runs through the strongest zone of mylonitization. Considering the general geometry of the shear zone, it seems likely that the mylonite zone was at one time also present along the eastern (outer) limb over the site of the MTL.

These lines of evidence suggest the following interpretation for the geotectonic history of the MTL. Figure 9 schematically illustrates the vertical tectonic setting of the mylonitic rocks combined with the model for the tectonic generation of the MTL proposed by Ichikawa (1970). In mid-Cretaceous time, syntectonic, metatexitic emplacement of the Hiji gneiss occurred, followed by deep-seated sinistral quasi-plastic (QP) shear movement with a minor amount of vertical-slip (Fig. 9a). Also at this stage, high pressure metamorphism probably took

place as a result of underthrusting of the oceanic plate along the Benioff zone (Miyashiro 1972). Sinistral movement along the shear zone can possibly be ascribed to oblique subduction of the Kula plate (Uyeda & Miyashiro 1974) which was moving towards the NNW. Geological evidence of a relative uplift of the Sambagawa belt to the Izumi Group is found in some places in SW Japan (Ichikawa 1980). The uplift of the Sambagawa belt may be inferred to be produced by downward stacking of material onto a descending plate below the Sambagawa metamorphic rocks. Thus the mylonitic rocks along eastern limb of the whole shear zone became eroded together with metamorphic rocks equivalent to those of the Ryoke belt in late Cretaceous time. On the other hand, no clast of crystalline schist has been found within the Izumi Group suggesting that the Sambagawa rocks were not exposed at the surface near the MTL at that time (Ichikawa 1980). In Paleogene time, the Sambagawa and the Ryoke metamorphic rocks came to be juxtaposed together near the present erosion level when cataclastic deformation was imposed (Fig. 9c). At this stage, the eastern limb of the whole shear zone was almost lost by erosion. The loss of rocks above the Sambagawa metamorphic rocks, probably equivalent to those of the Ryoke belt, has been assumed by several authors (e.g. Yabe 1963, Ichikawa 1964, 1970). As pointed out by them, many geological and sedimentological observations can be accounted for in this way.

CONCLUSIONS

(1) Toward the MTL, the mean size of quartz grains, a good indicator of mylonitization, decreases from 0.5 mm to less than 0.1 mm in the study area. There is no significant change of aspect ratio of recrystallized quartz grains.

(2) Mixed ductile–brittle behaviour for each mineral and whole rock indicates that cataclastic deformation overprinted the foliated mylonitic rocks close to the MTL.

(3) Development of fluxion banding (Sm) seems to be remarkably dependent on the existence of K-feldspar which forms a myrmekitic aggregate. The presence of pressure shadows coexisting with 'mixed' matrix suggests that the deformation took place accompanying intercrystalline diffusive mass transfer.

(4) Asymmetric microstructures in foliated mylonitic rocks such as asymmetric pressure shadows, displaced broken grains, mica 'fish' and oblique incremental elongation fabric all imply a sinistral sense of shearing.

(5) The above-mentioned asymmetric microstructures and the attitude of the stretching lineation (Lm) demonstrate that the shear movement of the mylonite zone was essentially sinistral strike-slip with a minor vertical-slip component.

(6) Before the formation of the present MTL, defined as the contact of the Hiji gneiss and the Sambagawa metamorphic rocks, the Ryoke belt as well as the mylonite zone extended more easterly beyond the line of the present MTL, forming part of the hangingwall above the subduction interface which generated the Sambagawa metamorphic rocks. The MTL cuts the mylonite zone longitudinally in the middle part and its eastern limb has probably been eroded out together with metamorphic rocks equivalent to those of the Ryoke belt. It was probably accomplished by the movement of the Sambagawa belt relative to the Ryoke belt.

Acknowledgements—I wish to express my sincere thanks to Prof. S. Mizutani of Nagoya University for valuable suggestions during the course of this work. I am much indebted to Prof. Y. Saka of Waseda University, Prof. T. Uemura of Niigata University and two anonymous reviewers for critical reading of the manuscript and for helpful comments. Thanks are also due to Mr. F. Yogo and Mr. M. Rikita for preparation of thin sections. This work was supported partly by the Annual Project organized by Waseda University 1983 (No. 58A-26).

REFERENCES

Bell, T. H. & Etheridge, M. A. 1973. Microstructure of mylonites and their descriptive terminology. *Lithos* **6**, 337–348.

Berthé, D., Choukroune, P. & Jegouzo, P. 1979. Orthogneiss, mylonite and non-coaxial deformation of granites: the example of the South Armorican Shear Zone. *J. Struct. Geol.* **1**, 31–42.

Elliott, D. 1973. Diffusion flow laws in metamorphic rocks. *Bull. geol. Soc. Am.* **84**, 2645–2664.

Etchecopar, A. 1974. Simulation par ordinateur de la déformation progressive d'un aggregat polycristallin. Etude du développement de structures orientées par écrasement et cisaillement. Ph.D. thesis. Université de Nantes, France.

Etchecopar, A. 1977. A plane kinematic model of progressive deformation in a polycrystalline aggregate. *Tectonophysics* **39**, 121–139.

Etheridge, M. A. & Wilkie, J. C. 1979. Grainsize reduction, grain boundary sliding and the flow strength of mylonites. *Tectonophysics* **58**, 159–178.

Ghosh, S. K. 1975. Distortion of planar structures around rigid spherical bodies. *Tectonophysics* **28**, 185–208.

Hanmer, S. K. 1982. Microstructure and geochemistry of plagioclase and microcline in naturally deformed granite. *J. Struct. Geol.* **4**, 197–213.

Hara, I., Yamada, T., Yokoyama, S., Arita, M. & Hiraga, Y. 1977. Study on the southern marginal shear belt of the Ryoke metamorphic terrain—Initial movement picture of the Median Tectonic Line. *Earth Sci. (Chikyu Kagaku)* **31**, 204–217*.

Hara, I., Shyoji, K., Sakurai, Y., Yokoyama, S. & Hide, K. 1980. Origin of the Median Tectonic Line and its initial shape. *Mem. geol. Soc. Japan* **18**, 27–49.

Hashimoto, M. 1957. On the basic plutonic rocks of Miwa and Inasato District, Nagano Prefecture, Central Japan. *Bull. natn. Sci. Mus.* **3**, 137–155.

Hayama, Y., Miyagawa, K., Nakajima, W. & Yamada, T. 1963. The Kashio Tectonic Zone, Urakawa to Wada area, Central Japan. *Earth Sci. (Chikyu Kagaku)* **66**, 23–31*.

Hayama, Y. & Yamada, T. 1980. Median Tectonic Line at the stage of its origin in relation to plutonism and mylonitization in the Ryoke belt. *Mem. geol. Soc. Japan* **18**, 5–25.

Hayase, I. & Ishizaka, K. 1967. Rb–Sr dating on the rocks in Japan—I. South Western Japan. *J. Japan. Ass. Mineral. Petrol. Econ. Geol.* **58**, 201–212*.

Higgins, M. W. 1971. Cataclastic rocks. *Prof. Pap. U.S. geol. Surv.* **687**.

Ichikawa, K. 1964. Tectonic status of the Honshu Major Belt in Southwest Japan during the Early Mesozoic. *J. Geosci., Osaka City Univ.* **8**, 71–107.

Ichikawa, K. 1970. Some geotectonic problems concerning the Paleozoic–Mesozoic geology of Southwest Japan. In: *Island Arc and Ocean* (edited by Hoshino, M. & Aoki, H.) Tokai Univ. Press, 193–200*.

Ichikawa, K. 1980. Geohistory of the Median Tectonic Line of southwest Japan. *Mem. Geol. Soc. Japan*, No. 18, 187–212.

Ishizaka, K. 1966. A geochronological study of the Ryoke metamorphic terrain in the Kinki district, Japan. *Mem. Coll. Sci., Univ. Kyoto, Ser. B*, **33**, 69–102.

Kagami, H. 1973. A Rb–Sr geochronological study of the Ryoke granites in Chubu district, Central Japan. *J. geol. Soc. Japan* **79**, 1–10.

Kanisawa, S. 1961. Ryoke plutonic rocks of Takato district, Nagano Prefecture. *J. Japan. Ass. Mineral. Petrol. Econ. Geol.* **46**, 111–118*.

Kawachi, Y., Yuasa, M. & Katada, M. 1983. *Geology of the Ichinose District.* Quadrangle Series, scale 1:50,000, Geol. Surv. Japan, 1–70*.

Kerrich, R., Allison, I., Barnett, R. L., Moss, S. & Starkey, J. 1980. Microstructural and chemical transformations accompanying deformation of granite in a shear zone at Mieville, Switzerland: with implications for stress corrosion cracking and superplastic flow. *Contr. Miner. Petrol.* **73**, 221–242.

Kosaka, K. 1980. Fault-related fabrics of granitic rocks. *J. Fac. Sci., Univ. Tokyo, Sec. II* **20**, 77–115.

Lister, G. S. & Snoke, A. W. 1984. S-C mylonites. *J. Struct. Geol.* **6**, 617–638.

Masuda, T. & Fujimura, A. 1981. Microstructural development of fine-grained quartz aggregates by syntectonic recrystallization. *Tectonophysics* **72**, 105–128.

Miyashiro, A. 1961. Evolution of metamorphic belts. *J. Petrol.* **2**, 277–311.

Miyashiro, A. 1972. Metamorphism and related magmatism in plate tectonics. *Am. J. Sci.* **272**, 629–656.

Ono, A. 1981. Geology of the Takato–Kashio area. Ryoke belt, central Japan. *J. geol. Soc. Japan* **87**, 249–257*.

Ramsay, J. G. & Graham, R. H. 1970. Strain variation in shear belts. *Can. J. Earth Sci.* **7**, 786–813.

Ryoke Research Group 1972. The mutual relations of the granitic rocks of the Ryoke metamorphic belt in Central Japan. *Earth Sci. (Chikyu Kagaku)* **26**, 205–216*.

Schoneveld, C. 1977. A study of some typical inclusion patterns in strongly paracrystalline rotated garnets. *Tectonophysics* **39**, 453–471.

Shelley, D. 1964. On myrmekite. *Am. Mineral.* **49**, 41–52.

Sibson, R. H. 1977. Fault rocks and fault mechanisms. *J. geol. Soc. Lond.* **133**, 191–213.

Sibson, R. H., White, S. H. & Atkinson, B. K. 1981. Structure and distribution of fault rocks in the Alpine Fault Zone, New Zealand. In: *Thrust and Nappe Tectonics* (Edited by McClay, K. R. & Price, N. J.). *Spec. Publs geol. Soc. Lond.* **9**, 197–210.

Simpson, C. & Schmid, S. M. 1983. An evaluation of criteria to deduce the sense of movement in sheared rocks. *Bull. geol. Soc. Am.* **94**, 1281–1288.

Sugiyama, R. 1939. Studies on the rocks developed along the so-called 'Median Line'—I. *J. geol. Soc. Japan* **46**, 169–187**.

Suwa, K. 1973. Metamorphic rocks occurring along the Median Tectonic Line in the Japanese Islands: Ryoke and Sambagawa metamorphic belts. In: *Median Tectonic Line* (edited by Sugiyama, R.), Tokai University Press, 221–238*.

Takagi, H. 1982. On the definition of mylonite and the classification of mylonitic rocks. *Gakujutsu Kenkyu (Scientific Res.), School Educ., Waseda Univ. (Biol. & Geol.)* **31**, 49–57*.

Takagi, H. 1983. Cataclastic deformation on mylonitic rocks along the Median Tectonic Line—Examples in Kami-Ina district, Nagano Prefecture. *Gakujutsu Kenkyu (Scientific Res.), School. Educ., Waseda Univ. (Biol. & Geol.)* **32**, 47–60*.

Takagi, H. 1984. Mylonitic rocks along the Median Tectonic Line in Takato–Ichinose area, Nagano Prefecture. *J. geol. Soc. Japan* **90**, 81–100*.

Takagi, H. & Ito, M. 1985. Asymmetric microstructures in mylonites as indicators of the sense of movement in ductile shear zone along the MTL. *Abstr. 92nd Ann. Meeting, geol. Soc. Japan*, 493.**

Tanaka, K. & Nozawa, T. (eds.) 1977. *Geology and Mineral Resources of Japan* (3rd Edn). Geol. Surv. Japan.

Uyeda, S. & Miyashiro, A. 1974. Plate tectonics and the Japanese Islands: a synthesis. *Bull. geol. Soc. Am.* **85**, 1159–1170.

Watts, M. J. & Williams, G. D. 1979. Fault rocks as indicators of progressive shear deformation in the Guingamp region, Brittany. *J. Struct. Geol.* **1**, 323–332.

White, S. 1975. Estimation of strain rates from microstructures. *J. geol. Soc. Lond.* **131**, 577–583.

Yabe, H. 1963. Probable position of the outer wing of the Ryoke metamorphics in Southwest Japan. *J. Geogr. Tokyo* **72**, 110–114*.

Yamana, S., Honma, H. & Kagami, H. 1983. Nd and Sr isotopic study on the granitic rocks and the basic rocks of the Ryoke belt. *Magma* **67**, 135–142**.

*In Japanese with English abstract.

**In Japanese.